Spin correlations in a simple cubic antiferromagnet $L1_2$-type Pt_3Fe

2009 J. Phys.: Condens. Matter 21 124209

(http://iopscience.iop.org/0953-8984/21/12/124209)

J. Phys.: Condens. Matter **21** (2009) 124209 (5pp) doi:10.1088/0953-8984/21/12/124209

Spin correlations in a simple cubic antiferromagnet $L1_2$-type Pt_3Fe

Ryusuke Matsui and Yorihiko Tsunoda

School of Science and Engineering, Waseda University, 3-4-1 Ohkubo, Shinjuku, Tokyo 169-8555, Japan

Received 14 September 2008, in final form 17 October 2008
Published 25 February 2009
Online at stacks.iop.org/JPhysCM/21/124209

Abstract

Magnetic diffuse scattering of neutrons was studied for a simple cubic antiferromagnet $L1_2$-type Pt_3Fe alloy in a paramagnetic phase. In order to visualize the physics, the data were analyzed using a localized spin model and effective exchange coupling parameters were determined. The result shows a special feature of exchange couplings; the first neighbor coupling constant J_1 has almost the same value and the same sign as that of the second neighbor J_2. This fact explains well coexistence of the (1/2 1/2 0)-type and (1/2 0 0)-type magnetic structures in the low temperature phase of Pt_3Fe alloy.

1. Introduction

Fcc $Pt_{100-X}Fe_X$ ($X > 1$) alloys show a rich variety of magnetism with changes of Fe concentrations and their atomic configurations. Disordered alloys always show ferromagnetic long range order although a weak antiferromagnetic component coexists [1]. Among these alloys, the magnetism of ordered $Pt_{75}Fe_{25}$ alloy is very interesting. A pure antiferromagnetic long range order develops. The ordered $Pt_{75}Fe_{25}$ alloy has an $L1_2$-type structure, in which the corner sites are occupied by Fe atoms and the face center sites by Pt atoms, respectively. (Hereafter we refer an atomic ordered state of $Pt_{75}Fe_{25}$ alloy as Pt_3Fe.) Bacon and Crangle [2] studied the magnetism of Pt–Fe alloys with relevant Fe concentration range using powder and single crystal specimens by neutron diffraction. For a $Pt_{2.93}Fe_{1.07}$ alloy (ordered $Fe_{73.3}Fe_{26.7}$ alloy) which showed antiferromagnetic long range order below $T_N = 160$ K, they found an abrupt change of the antiferromagnetic (1/2 1/2 0) peak intensity around $T_S = 110$ K. Below T_S, a new peak appears at the (1/2 0 0) reciprocal lattice point (RLP) with the decrease of the (1/2 1/2 0) peak intensity. They proposed a spin structure model for Pt_3Fe alloy as shown in figure 1. Since Pt atoms carry no magnetic moments, Pt_3Fe alloy is considered to be a simple cubic antiferromagnet. In the $L1_2$-type structure, excess or mis-sitting Fe atoms occupy at the face center positions. The nearest neighbor Fe moments in the face centered plane couple ferromagnetically and the second neighbor Fe moments antiparallel. Thus, the Bacon's model assumes existence of mis-sitting Fe atoms to explain the (1/2 0 0)-type structure in the low temperature phase of the stoichiometric Pt_3Fe alloy and is an inhomogeneous model with a mixture of the (1/2 1/2 0)-type and the (1/2 0 0)-type structures. Kohgi and Ishikawa [3] have studied magnon dispersion relations for a $Pt_{3.10}Fe_{0.90}$ single crystal which showed a weak (1/2 0 0) magnetic Bragg peak in addition to the ordinary (1/2 1/2 0) magnetic peak at the lowest temperature. The data were analyzed under the localized Heisenberg spin model and effective exchange coupling constants were determined.

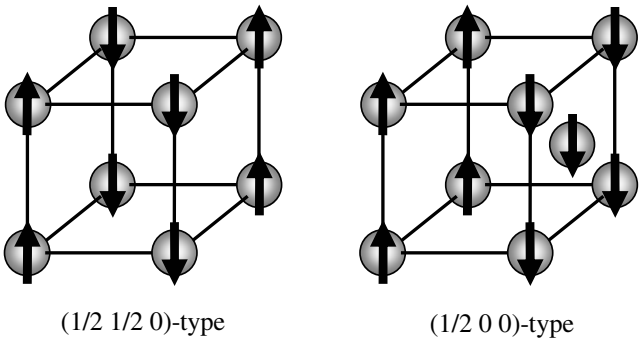

Figure 1. The (1/2 1/2 0)-type and (1/2 0 0)-type magnetic structures reported by Bacon and Crangle [2].

On the other hand, Vinokurova *et al* [4] studied the magnetism of $Pt_{3-X}Fe_{1+X}$ ($X = 0.12$ and 0.28) using neutron diffraction. From the analogy of their results, they suggested a uniform model which comes from the degeneracy of two magnetic structures at the low temperature phase of Pt_3Fe alloy. Furthermore, Kulikov *et al* [5] calculated the band

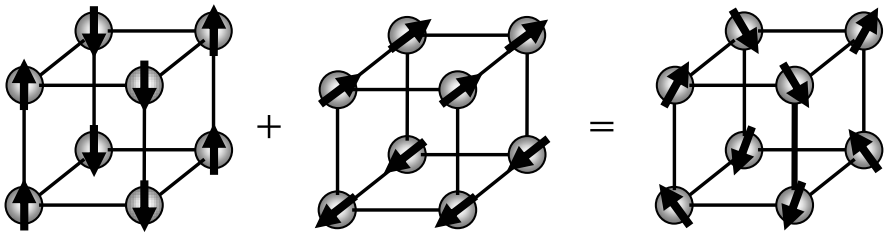

Figure 2. Non-collinear spin structure with both components of the (1/2 1/2 0)-type and (1/2 0 0)-type magnetic structures.

structure of paramagnetic Pt_3Fe alloy and pointed out the possibility of the nesting feature of electron and hole Fermi surfaces to explain the antiferromagnetism of Pt_3Fe ordered alloy. Unfortunately, however, experimental evidence to verify the degenerate spin-density-wave (SDW) formation had not been reported in the system. Recently, one of the present author and colleague [6] studied the magnetic structure of Pt_3Fe ordered alloy using a single domain single crystal under a uniaxial stress and demonstrated the validity of the uniform model with a non-collinear magnetic structure for the low temperature phase of Pt_3Fe alloy. The resultant structure is shown in figure 2. They pointed out that the magnetic phase transition at T_S in the Pt_3Fe alloy is one of crossover points of the antiferromagnetic spin correlations in the Pt–Fe system [7].

Among the simple cubic antiferromagnetic structures, ferro- and antiferromagnetic first neighbor spin couplings coexist in both the (1/2 1/2 0)-type and (1/2 0 0)-type structures, suggesting existence of spin frustration. In the present measurements, magnetic diffuse scattering of neutrons was studied in the paramagnetic phase using a single crystal specimen of Pt_3Fe alloy to investigate the frustrating spin correlations in the simple cubic antiferromagnet. For the magnetism of metallic system such as the Pt_3Fe, the itinerant electron treatment would be better, but the experimental data were analyzed using a localized spin model to understand the physics visually and to compare the results with the values reported by the previous authors [3].

2. Sample preparation and experiment

Single crystal of $Pt_{75}Fe_{25}$ was grown by Bridgman method in a furnace with a carbon electrode under an Ar-gas atmosphere. This specimen has a volume of about 2 cm^3. The cooling speed of the furnace was about 200 °C min^{-1} around 1000 °C. The furnace cooled sample already shows rather good $L1_2$-type chemical order. However, to improve the atomic long range order the single crystal was annealed at 1000 °C for 10 days in Ar(+5%H_2)-gas atmosphere and slowly cooled down to room temperature.

Neutron scattering measurements were performed at the T1-1 triple axis spectrometer installed in a thermal guide of JRR-3M, Tokai, Japan. The incident neutron energy of 13.5 meV was used for all of the measurements. The $\lambda/2$ component of the incident neutron was eliminated using pyrolytic graphite filter. Temperature of the specimens was controlled in a refrigerator unit operated by the Solvay cycle.

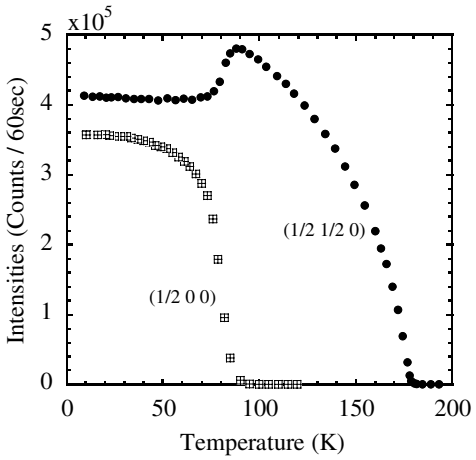

Figure 3. Temperature variations of the magnetic Bragg peak intensities at (1/2 1/2 0) and (1/2 0 0).

3. Experimental data

The temperature variations of the (1/2 1/2 0) and (1/2 0 0) magnetic Bragg peak intensities for our sample are given in figure 3. Our Pt_3Fe single crystal showed a Néel temperature $T_N = 180$ K. To study the spin correlations of the simple cubic antiferromagnet, we carried out the neutron diffuse scattering experiments in the paramagnetic phase at 200 K (=1.11T_N). Thus, it is not necessary to consider anisotropy of the scattering intensities due to the magnetic domain distribution. In figure 4, the total scattering intensity contour maps on the (0 0 1) and (1 $\bar{1}$ 0) scattering planes are shown. These maps were drawn using 1740 and 1428 measuring points in total respectively and scattered neutrons were accumulated for 30 s at each point. In this measurement, the analyzer crystal was removed to obtain the data of all scattering processes integrated over energies. In these figures, solid lines indicate the reciprocal lattice frame of a simple cubic structure, and broken lines show the middle of this reciprocal lattice. In the (0 0 1) scattering plane, the magnetic Bragg peak positions of the (1/2 1/2 0)-type and (1/2 0 0)-type structures exist, while the (1 $\bar{1}$ 0) scattering plane includes the Bragg peak positions of three main structures (0 0 1/2)-, (1/2 1/2 0)- and (1/2 1/2 1/2)-types of the simple cubic antiferromagnet. Diffuse scattering intensity distributes around the (1/2 1/2 0) and (1/2 0 0) RLPs, which correspond to the high temperature magnetic phase and the component of the low temperature phase, respectively, but no peak around the (1/2 1/2 1/2) RLP.

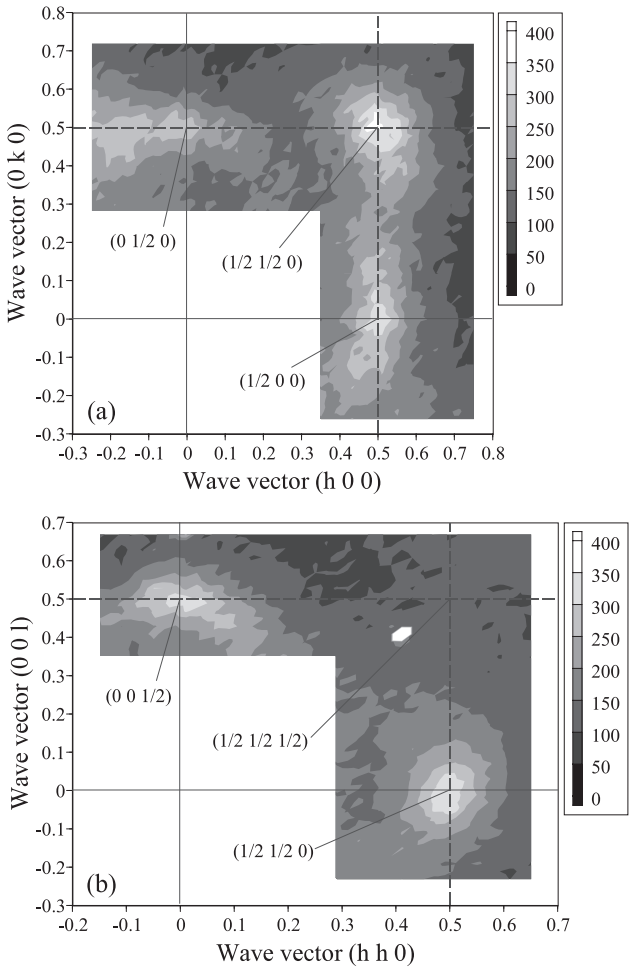

Figure 4. Diffuse scattering intensity contour maps on the (0 0 1) and (1 $\bar{1}$ 0) scattering planes studied without analyzer crystal at 200 K (1.11 T_N). (a) The (0 0 1) scattering plane and (b) the (1 $\bar{1}$ 0) scattering plane. A sharp peak at (0.41 0.41 0.41) would be due to multiple scattering.

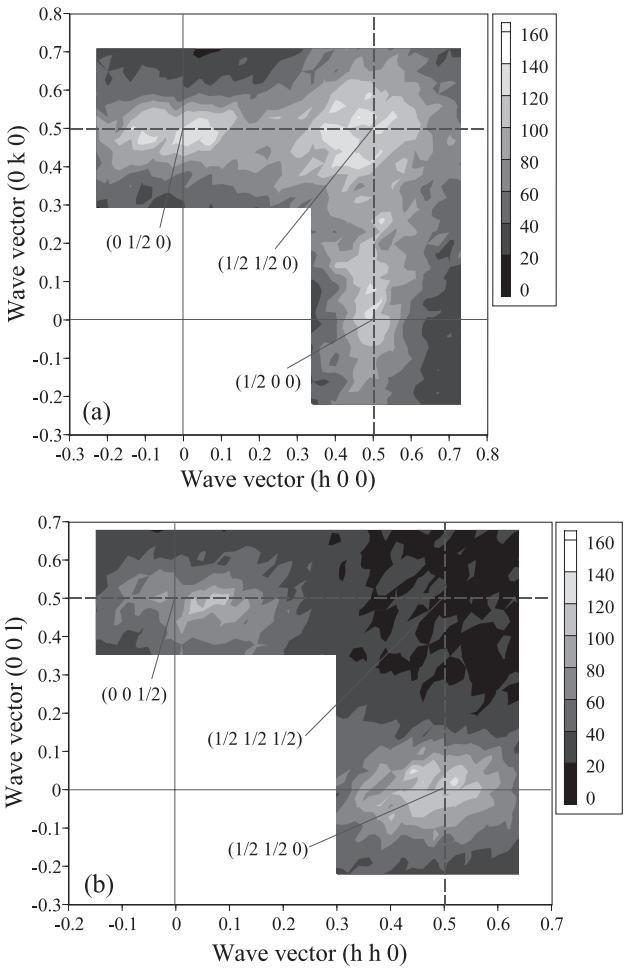

Figure 5. Inelastic diffuse scattering intensity contour maps on the (0 0 1) and (1 $\bar{1}$ 0) scattering planes studied at 200 K in the constant-E mode of $\Delta E = 5$ meV. (a) The (0 0 1) scattering plane and (b) the (1 $\bar{1}$ 0) scattering plane.

Furthermore, the diffuse scattering intensity extends along the broken lines on the (0 0 1) scattering plane. Inelastic neutron scattering measurements in the constant-E mode of operation at $\Delta E = 5$ meV were also studied using the analyzer crystal and the intensity contour maps are given in figure 5. These maps were drawn using 750 and 841 measuring points in the (0 0 1) and (1 $\bar{1}$ 0) scattering planes, respectively and each datum was taken for 90 s. The results are very similar to those for the total scattering intensities, suggesting that the spin correlations are frequency independent.

These data indicate that the spin correlations of the (1/2 1/2 0)-type and (1/2 0 0)-type coexist, however, the simplest antiferromagnetic spin correlation with the (1/2 1/2 1/2)-type does never exist in the paramagnetic phase at $T/T_N = 1.11$.

4. Data analysis

To understand these diffuse scattering patterns, we tried to reproduce the intensity contour maps in the (0 0 1) and (1 $\bar{1}$ 0) scattering planes (figure 4) using a simple classical Heisenberg model under the random-phase approximation (RPA) treatment. Since the data for figure 4 were obtained without using analyzer, scattering processes integrated over all energies were included. Strictly saying, since the incident neutron energy was rather low ($E_0 = 13.5$ meV) and the Q-space we have measured was limited to the regions with rather small scattering vector, inelastic scattering with large energy transfer was prohibited due to the energy–momentum conservation law. However, contribution of high energy transfer processes would be very low in the short measuring time (30 s). Thus, we assume that the data including the scattering processes integrated over all energies. Then, we can consider here only the space correlations of spins.

Neutron scattering cross section above the phase transition temperature associated with a spin fluctuation is represented using a static susceptibility

$$I(\mathbf{k}) \propto \chi(\mathbf{q}).$$

The static susceptibility is given by the following equation under the RPA

$$\chi(\mathbf{q}) \propto \frac{1}{\Delta - (J(\mathbf{q}_0) - J(\mathbf{q}))}$$

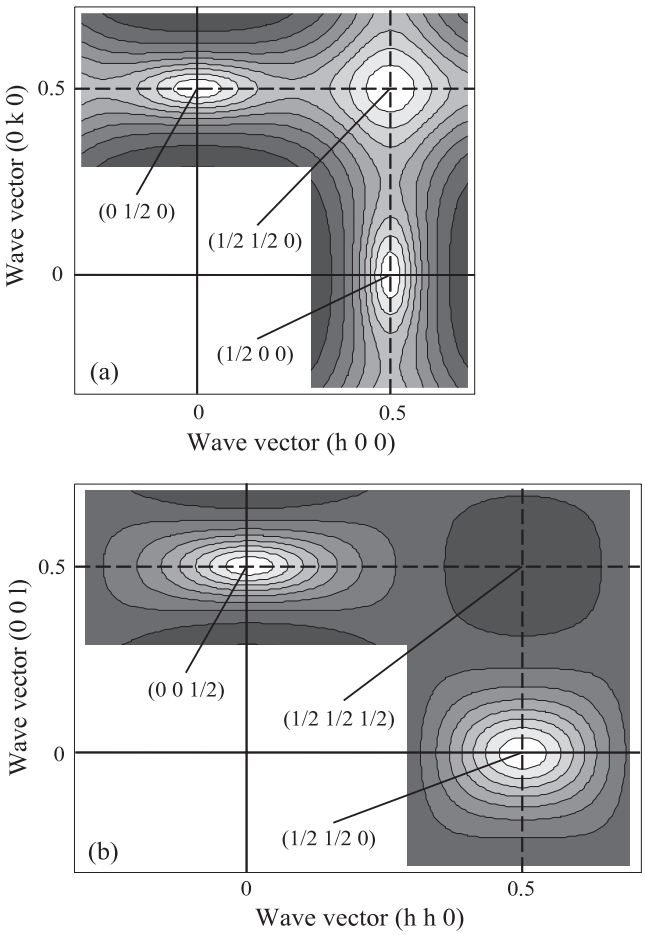

Figure 6. Calculated diffuse scattering intensity contour maps on the (0 0 1) and (1 $\bar{1}$ 0) scattering planes using the parameters given in the text. (a) The (0 0 1) scattering plane and (b) the (1 $\bar{1}$ 0) scattering plane.

where, $\Delta = k_B(T - T_N)$ represents the degree of the deviation from Néel temperature. The wavevector $\mathbf{q}_0$ is the characteristic wavevector when the system is in the ground state. $J(\mathbf{q})$ represents the Fourier transform of the interaction matrix. The exchange interactions from the first to sixth neighbor atoms were taken into consideration and described as from J_1 to J_6, respectively.

Figure 6 shows the calculated intensity contour maps in the (0 0 1) and (1 $\bar{1}$ 0) scattering planes using the best fitting values of J_n as the parameters. The calculated intensity maps reproduce well the main features of the experimental data such as the diffuse peak positions and extending direction of diffuse scattering. Since we did not measure the absolute value of the intensities, only the ratios of the exchange parameters were determined. The ratios of the best fitting parameters determined here were $J_1{:}J_2{:}J_3{:}J_4{:}J_5{:}J_6 = -1{:}-0.9{:}-0.27{:}0.1{:}-0.02{:}-0.03$ (where $J_n > 0$ indicates ferromagnetic coupling). In course of calculations, we found that various attempts considering up to the 3rd neighbor interaction J_3 always failed to reproduce the observed intensity maps, indicating that the fourth neighbor exchange interaction J_4 plays an important role to reproduce the experimental data. On the other hand, J_5 and J_6 hardly contribute to reproduce the experimental data.

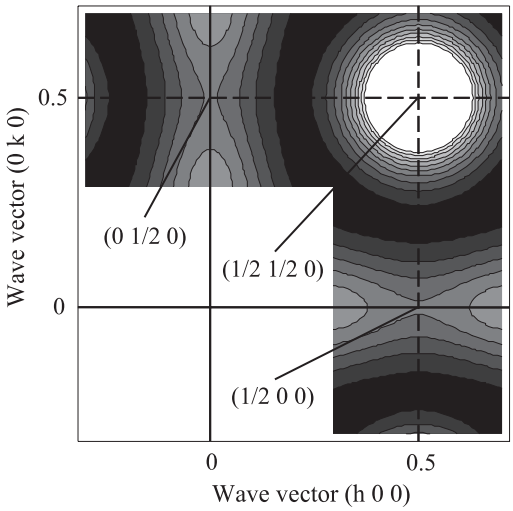

Figure 7. Calculated diffuse scattering intensity contour maps on the (0 0 1) scattering plane using the exchange coupling parameters reported by Kohgi and Ishikawa [3].

Table 1. Comparison of the exchange fitting parameters up to sixth neighbor atoms. Exchange parameters for $Pt_{3.10}Fe_{0.90}$ are normalized to the value of J_1 for comparison.

	J_1	J_2	J_3	J_4	J_5	J_6
Pt_3Fe (present data)	−1	−0.9	−0.27	0.1	−0.02	−0.03
$Pt_{3.10}Fe_{0.90}$ [3]	1	−0.56	0.48	0.18	0.03	−0.12

Note that the dynamical susceptibility $\chi(\mathbf{q}, \omega)$ ($\hbar\omega = 5$ meV) also shows almost the similar spin correlations to the static susceptibility $\chi(\mathbf{q})$.

5. Discussion

Kohgi and Ishikawa [3] determined the exchange coupling constants using their experimental data of magnon dispersion relations for $Pt_{3.10}Fe_{0.90}$ single crystal under the Heisenberg localized spin model. In addition to the (1/2 1/2 0) Bragg peak, their sample showed very weak (1/2 0 0) magnetic peak (∼1% of (1/2 1/2 0)) at the lowest temperature (∼5 K) and was slightly different from our stoichiometric alloy Pt_3Fe, but fundamental magnetic properties should be the same. Thus, it would be meaningful to compare the results for both systems. Exchange coupling parameters reported are compared with our results in table 1. Exchange coupling parameters determined here are completely different from those of the previous authors. The differences are not only the absolute values but even their signs. The reason of these differences could not be ascribed to the small difference of the Fe concentration of the alloys.

The present experimental data indicate that both the (1/2 1/2 0)-type and (1/2 0 0)-type spin correlations coexist even in the paramagnetic phase, suggesting that the (1/2 1/2 0)-type spin structure and the (1/2 0 0)-type structure degenerate energetically. In order to confirm this point, we calculated magnetic energies for both structures. Under the

localized spin model, the Hamiltonian is described as

$$H = -2\sum_{\langle i,j\rangle} J_{ij} S_i S_j - D\sum_i S_{iz}^2,$$

where J_{ij} is the effective exchange interactions between ith and jth iron atoms and D is the phenomenological anisotropy constant. Only the exchange interactions between iron atoms were considered because platinum atoms have no magnetic moment as previously mentioned. If we assume the two magnetic states, the (1/2 1/2 0)-type and (1/2 0 0)-type structures, are energetically degenerate, following equations should be satisfied when we take the exchange coupling constants up to the fourth order. This assumption would be justified because the diffuse scattering patterns are insensitive to the fifth and sixth neighbor interactions.

$$2J_1 + 4J_2 - 8J_3 - 6J_4 = -2J_1 + 4J_2 + 8J_3 - 6J_4.$$

Then, we obtain the simple equation:

$$J_1 = 4J_3.$$

Furthermore, the total magnetic energy should be negative. Using above condition, we obtain

$$2J_2 - 3J_4 < 0.$$

Our exchange coupling constants determined here almost satisfy these conditions, but those of Kohgi and Ishikawa do not satisfy the first condition. In order to check this point, we calculated the susceptibility $\chi(\mathbf{q})$ using the exchange parameters reported by these authors and compared it with our results. The calculated $\chi(\mathbf{q})$ for the (0 0 1) scattering plane is given in figure 7. Their sample was non-stoichiometric and a very weak (1/2 0 0) magnetic Bragg peak was observed at the lowest temperature. The weak diffusive peak around the (1/2 0 0) RLP may be an indication of the appearance of the (1/2 0 0)-type structure. However, the extending direction of diffuse scattering is completely different from our experimental and calculated data, for which diffuse scattering extends along the direction from the (1/2 0 0) to (1/2 1/2 0) RLPs.

The exchange coupling constants determined here have a special feature. The first neighbor coupling constant J_1 has almost the same value and the same sign as that of the second neighbor J_2 although the second neighbor distance is $\sqrt{2}$ times larger than the first neighbor distance. That is to say, both the first and second neighbor spins favor antiferromagnetic coupling with the same strength. For the simple cubic lattice, these interactions conflict each other. However, the number of second neighbor atoms is more than that of the first neighbor atoms, resulting that the structure with antiferromagnetic coupling at the second neighbor spins, the (1/2 1/2 0)-type and/or the (1/2 0 0)-type structure, is stabilized but never stabilized the (1/2 1/2 1/2)-type structure because all of the second neighbor spins couple ferromagnetically for the latter. The (1/2 1/2 0)-type and (1/2 0 0)-type structures look like a competing system of ferro- and antiferromagnetic couplings if we consider the first neighbor spin coupling only, but this is not true. The ferromagnetic coupling of the first neighbor spins in the (1/2 1/2 0)-type and (1/2 0 0)-type structures occurs as a result of conflicting spin couplings of the first and second neighbor antiferromagnetic interactions. In this sense, we can regard the Pt_3Fe ordered alloy as a kind of a frustrating system. This is consistent with the results of our previous work [6] in which we reported that the T_N of the Pt_3Fe alloy sensitively increased under the uniaxial stress because the tetragonal lattice deformation suppresses the spin frustrations. Note that the equal values of J_1 and J_2 are not the necessary condition for the degeneracy of the (1/2 1/2 0)-type and (1/2 0 0)-type structures. This feature rather seems to be accidental for this system.

As shown in figures 4 and 5, the total diffuse scattering and inelastic scattering intensities show broad peaks at the same positions around the (1/2 0 0) and (1/2 1/2 0) RLPs, indicating that the space correlations of spins are independent to frequencies. That is to say, above the transition temperature, spins are dynamically fluctuating with various frequencies as clusters keeping with space correlations. This seems to be a characteristic common to metallic frustrating spin systems such as the geometrical frustration systems [8] and spin-glass alloys [9].

Kulikov *et al* [5] reported in their band calculations that the two different spin-density-waves (SDWs) with the wavevector $Q_1 = (2\pi/a)(1/2\ 1/2\ 0)$ and $Q_2 = (2\pi/a)(1/2\ 0\ 0)$ coexist for Pt_3Fe ordered alloy and they calculated the static susceptibility $\chi(\mathbf{q})$ along the major crystallographic directions in the paramagnetic phase. The susceptibility showed the maximum values at the M and X points which correspond to the (1/2 0 0) and (1/2 1/2 0) RLPs, respectively. The present experimental data are consistent with these calculations. In our data analysis, we used the localized spin model in order to visualize the physics easily. However, the theoretical result derived by Kulikov *et al* under the band calculation has just the same physical meanings as that the first neighbor coupling constant J_1 has almost the same value and the same sign as that of the second neighbor J_2 in the localized spin model.

References

[1] Tsunoda Y and Abe R 1997 *Phys. Rev.* B **55** 11507
[2] Bacon G E and Crangle J 1963 *Proc. R. Soc.* A **272** 387
[3] Kohgi M and Ishikawa Y 1980 *J. Phys. Soc. Japan* **49** 985
[4] Vinokurova L, Ivanov V, Kulatov E T, Pardavi-Horvath M and Svab E 1988 *J. Physique* **49** C8117
Vinokurova L, Ivanov V, Kulatov E T, Pardavi-Horvath M and Svab E 1989 *Acta Phys. Pol.* A **76** 381
[5] Kulikov N I, Kulatov E T and Yakhimovich S I 1985 *J. Phys. F: Met. Phys.* **15** 1127
[6] Yano S and Tsunoda Y 2007 *J. Magn. Magn. Mater.* **310** 1841
[7] Tsunoda Y, Tsuchiya D and Higashiyama Y 2003 *J. Phys. Soc. Japan* **72** 713
[8] Ballou R, Lelièvre-Berna E and Fåk B 1996 *Phys. Rev. Lett.* **76** 2125
[9] Tsunoda Y, Kunitomi N and Cable J W 1985 *J. Appl. Phys.* **57** 3753